

Real-Time and Label-Free Detection of the Prostate-Specific Antigen in Human Serum by a Polycrystalline Silicon Nanowire Field-Effect Transistor Biosensor

Yu-Wen Huang,[†] Chung-Shu Wu,[†] Cheng-Keng Chuang,[‡] See-Tong Pang,[‡] Tung-Ming Pan,^{*,§} Yuh-Shyong Yang,^{||} and Fu-Hsiang Ko^{*,†}

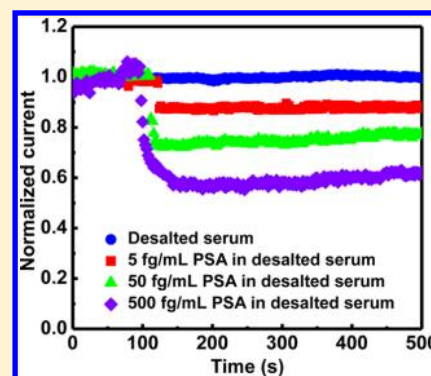
[†]Department of Materials Science and Engineering, Chiao-Tung University, Hsinchu 300, Taiwan

[‡]Division of Urology, Chang Gung Memorial Hospital, Taiyuan 333, Taiwan

[§]Department of Electronics Engineering, Chang Gung University, Taoyuan 333, Taiwan

^{||}Department of Biological Science and Technology, National Chiao Tung University, Hsinchu 300, Taiwan

ABSTRACT: In this research, we used a polycrystalline silicon nanowire field-effect transistor (poly-Si NWFET) as a biosensor that employs the sidewall spacer technique instead of an expensive electron beam lithography method. When compared with commercial semiconductor processes, the sidewall spacer technique has the advantages of simplicity and low cost. In this study, we employed a novel poly-Si NWFET device for real-time, label-free, and ultrahigh-sensitivity detection of prostate-specific antigen (PSA) in human serum. Since serum proteome is very complex containing high levels of salts and other interfering compounds, we hereby developed a standard operating procedure for real-sample pretreatment to keep a proper pH value and ionic strength of the desalted serum and also utilized Tween 20 to serve as the passivation agent by surface modification on the NWFET to reduce nonspecific binding for medical diagnostic applications. We first modified 3-aminopropyltriethoxysilane on the surface of a poly-Si nanowire device followed by glutaraldehyde functionalization, and the PSA antibodies were immobilized on the aldehyde terminal. While PSA was prepared in the buffers to maintain an appropriate pH value and ionic strength, the results indicated that the sensor could detect trace PSA at less than 5 fg/mL in a microfluidic channel. The novel poly-Si NWFET is developed as a diagnostic platform for monitoring prostate cancer and predicting the risk of early biochemical relapse.



Cancer is a major public health concern and represents a significant burden of disease in the world. Every year, tens of millions of people are diagnosed with cancer in their lifetimes, and more than half of the patients finally die of the metastatic disease. Prostate cancer is one of the most common malignant diseases among men worldwide and is the second leading cause of male cancer death in the United States.¹ The malignant neoplasms of the prostate gland are very slow growing, so that is why men over 50 are the most at risk. Risk factors like diet and genetics have been implicated in the development of prostate cancer. Since the discovery and characterization of prostate-specific antigen (PSA), as a screening tool for the prostate cancer in the 1980s, this disease can now be detected at a much earlier stage.² Early prostate cancer is usually localized and has no symptoms, while the cancer that has metastasized to other parts of the body may cause pain, especially from spread to the bones. Therefore, early detection of prostate cancer greatly increases the opportunity for successful treatment and curative surgery. PSA is a 33 kDa single-chain glycoprotein belonging to the kallikrein family of serine proteases.³ Serine protease is secreted exclusively by the epithelial cells of all types of the prostatic tissue and is a normal component of the seminal plasma.⁴ PSA is highly expressed by

normal prostatic epithelial cells and represents one of the most characterized tumor-associated antigens in prostate cancer.^{5–7} Today, PSA is the most widely used tumor marker worldwide for screening, diagnosing, and monitoring prostate cancer. Measurement of PSA in blood is the most sensitive marker available for monitoring the progression of prostate cancer and the response to therapy.

The definition of biosensors is “devices that use specific biochemical reactions mediated by isolated enzymes, immunosystems, tissues, organelles or whole cells to detect chemical compounds usually by electrical, thermal or optical signals” by the International Union of Pure and Applied Chemistry (IUPAC).⁸ Biosensors are analytical devices which apply for many different fields of environmental monitoring, military application, industrial process control, medicine requirements, and clinical diagnostics and can be capable of providing either qualitative or quantitative results.^{9,10} According to the principle of working methods, biosensors are often classified as being label-based detection and label-free detection.^{11,12} Label-based

Received: May 29, 2013

Accepted: July 11, 2013

Published: July 11, 2013

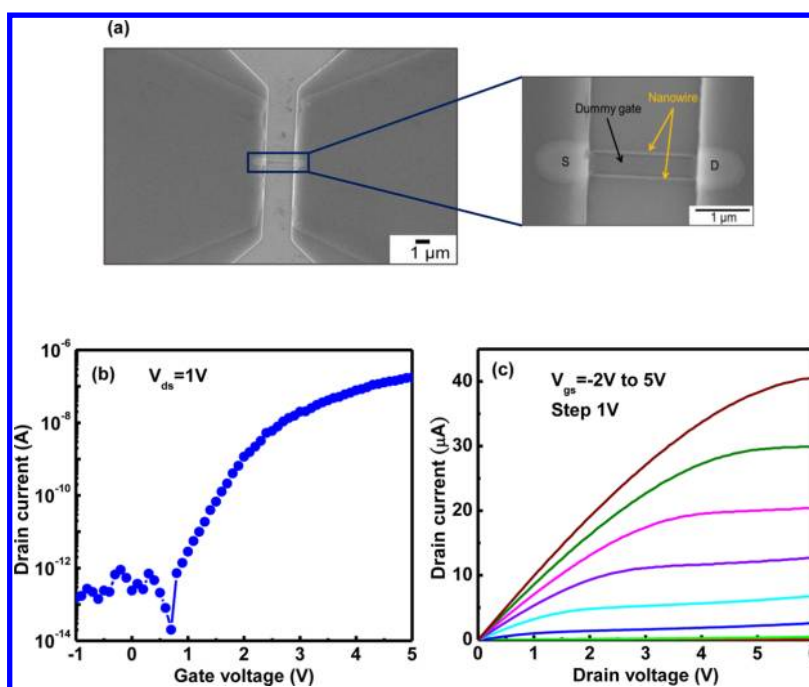


Figure 1. (a) SEM image of the poly-Si NWFET device. The yellow arrow indicates that the nanowire beside the dummy gate is 2 μm in length. (b) $I_{ds}-V_{gs}$ curve of the poly-Si NWFET device. (c) The $I_{ds}-V_{ds}$ curve depended on the V_{gs} varying from -2 to 5 V in 1 V steps.

technique requires labeling of molecules with labels such as fluorescence, radioactivity, luminescence, and epitope tags. Several detection methods are label-based such as DNA microarray^{13,14} and enzyme-linked immune sorbent assay (ELISA).¹⁵ Although the label-based assay has a lower detection limit, experimental procedures of these methods are more complex and difficult. Moreover, there are some synthetic challenges about the labeling strategies, multiple label issues, and may exhibit interference with the binding site. Thus, the development of sensitive, reliable, high-throughput, label-free detection techniques is now attracting significant attention. In recent years, label-free detection techniques are employed to many regions of research, such as surface plasmon resonance (SPR),¹⁶ quartz crystal monitor (QCM),¹⁷ microcantilevers (MC),^{18,19} and nanowire field-effect transistor (NWFET),²⁰ monitoring biomolecular interactions and simplifying the bioassays by eliminating the need for secondary reactants.

Field-effect transistor (FET) biosensors have the potential to be employed as rapid and low-cost screens for use in label-free electrical detection with the excellent specificity and highly sensitivity. The FET device is able to switch or control electricity very quickly. The gate voltage is employed by the back gate, utilizing the degenerated doped silicon substrate or a liquid gate, external electrode immersed in the aqueous solution. By changing the electrical voltage or potential between the source and the gate, electrical resistance between the source and the drain is manipulated. The applied voltage to the gate (more than a threshold voltage) can cause a raising or lowering of the current flowing through the drain to the source in a transistor. To date, nanoscaled detecting techniques have been used for application and research of the broad fields. A variety of NWFET biosensors have been applied for biological detection, such as cell-based FET devices, immunologically modified FET devices, and enzyme-functionalized FET devices.²¹ In general, immunologically modified FET devices are the most frequently utilized as biosensors. The antibodies

immobilized onto the surface of the FETs can be employed to measure the concentrations of the corresponding antigen. The direction of the conductance change indicates the presence of charge carriers in the semiconductive channel by the target antigen, and the magnitude of the variation depends on the interaction between antigen and antibody. For example, in an n-type NWFET, the negatively charged analytes like nucleic acids binding to the receptor-anchored NWFETs will cause the depletion of charge carriers in the current channel and thus give rise to the increasing current in the device. On the contrary, the devices bind to the positively charged molecules, resulting in a decrease in the current of an FET device originating from the accumulation of charge carriers. Therefore, the target analytes with charge carriers could be screened by the NWFETs.

A simple and low-cost method to fabricate polycrystalline silicon (poly-Si) NWFET has been previously reported for biosensing application.^{22–27} The poly-Si sidewall spacer technique was used to define the nanoscale patterns without expensive electron beam lithography systems. Furthermore, this FET biosensor exhibits a high sensitivity and excellent specificity and is able to detect target molecules rapidly and precisely. The resulting cancer statistics¹ mentioned that male persons suffering from prostate cancer are in an upswing each year. There are often no signs and symptoms of the prostate cancer in the early stages; however, it is the prime time for the treatment of localized prostate cancer. Besides, an elevated level of PSA in the patient after therapy is often an early indication of prostate cancer recurrence. Previous studies^{28,29} also demonstrated that the biochemical recurrence affects roughly 15–30% of men initially thought to be curable with localized treatment for prostate cancer. In this study, we proposed poly-Si NWFETs with high selectivity and sensitivity, real-time response, and label-free detection capabilities to screen the prostate cancer and predict its cancer recurrence.

MATERIALS AND METHODS

Fabrication of Poly-Si NFET Biosensors. The poly-Si NWFETs were fabricated at the National Nano Device Laboratories, Hsinchu, Taiwan, according to the previous research.^{22,26} The poly-Si NWFET biosensors were fabricated by utilizing 6 in. silicon (100) wafers as the device substrates. Then, the silicon wafers were capped with a 100 nm thick wet oxide, and thus deposited a 50 nm thick silicon nitride layer by low-pressure chemical vapor deposition. Next, a 100 nm thick TEOS oxide and 100 nm thick amorphous Si (α -Si) layer were deposited on the substrate to form the dummy gate. Subsequently, the device was annealed at 600 °C for 24 h in nitrogen ambient to transform the α -Si into the polycrystalline structure. Following this, the source/drain (S/D) implantation process was performed by phosphorus atoms with a dose of $1 \times 10^{15} \text{ cm}^{-2}$ at 15 keV. The S/D photoresist patterns were generated on the substrate by the lithography step; afterward, a reactive plasma etch step was performed to remove the poly-Si layer and to form the S/D regions. Eventually, after the process of anisotropic etching, the sidewall poly-Si NW channels were formed. The cross-sectional dimensions of poly-Si NWs could be controlled by the different etching times. The scanning electron microscopy (SEM) image of such a poly-Si NWFET device is shown in Figure 1a. The top-view SEM image indicated that the dummy gate was between source and drain electrodes, and the dimension of nanowire device was $0.08 \times 2 \mu\text{m}^2$ ($W/L = 0.08 \mu\text{m}/2 \mu\text{m}$).

Electrical Measurements of Poly-Si NWFET Devices.

The electrical measurements of poly-Si NWFET devices at room temperature were accomplished by employing current–voltage (I – V) measurement systems (HP4156C Precision Semiconductor Parameter Analyzer), probe station with the chamber (EVERBEING), and syringe pump (KD Scientific) connected with the microfluidic system. The dimension of fluidic channel is $5 \times 0.5 \times 0.1 \text{ mm}^3$. The 0.5 mm diameter inlet and outlet holes are located at the two ends of the channel. Samples with the PSA were passed through the NWFET sensor at a flow rate of $83 \mu\text{L}/\text{min}$ for 10 min. This continuous fluidic transport was operated by an automatic syringe pump. Generally, in the measurement of the drain current–gate voltage ($I_{\text{ds}}-V_{\text{gs}}$) curve, I_{ds} was measured at constant drain voltage ($V_{\text{ds}} = 1 \text{ V}$), whereas the gate voltage was swept from -1 to 5 V to evaluate the poly-Si NWFET performance in aqueous solution and to determine the biosensing parameters. The $I_{\text{ds}}-V_{\text{gs}}$ curve remained stable during the incubation. In a typical experiment, the determination of $I_{\text{ds}}-V_{\text{gs}}$ curve was repeated three times to make sure no further variation. In addition, in the measurement of the drain current–drain voltage ($I_{\text{ds}}-V_{\text{ds}}$) curve, the drain current was measured at several constant gate voltages (V_{gs} from -2 to 5 V with a 1 V step), while the V_{ds} was swept from 0 to 6 V to test electrical performance of such a poly-Si NWFET device.

Self-Assembly of Biomolecules on Poly-Si NWFET Devices. Before employing the sensor to measure biomolecules, the poly-Si NWFET device was modified to recognize the analytes by the self-assembly procedures. First, the FET sensor was cleaned in the mixture of ethanol and acetone (1:1). Second, the FET device was immersed into the 10% 3-aminopropyltriethoxysilane (APTES) solution for 30 min to form a self-assembled monolayer on the nanowire surface, washed with deionized (DI) water, and dried in nitrogen ambient. Third, the sample was heated on the hot plate at 120

°C for 10 min. The functionalization of the poly-Si NWFET device is performed using APTES to convert surface silanol groups (SiOH) to amines (NH₂). The amino groups are the terminal units from the device surface. Subsequently, the device was immersed in the 2.5% glutaraldehyde aqueous solution, prepared with phosphate-buffered saline (PBS), for 30 min, and then washed with DI water and dried in nitrogen ambient. At the processes, aldehyde groups from glutaraldehyde were connected to the amino groups to form the linker between the APTES and anti-PSA (PSA antibody). Finally, the chip was immobilized by immersing in the antibody solutions for 12 h and blocked the nonspecific reactive site by 1% bovine serum albumin (BSA) solution. Each step was rinsed by DI water and subsequently dried in nitrogen ambient.

Preparation of Human Serum. Serum is an ideal sample for biological applications because it provides a considerable amount of useful information about various disease hints released from the injured tissues. The serum proteome includes substances such as tumor markers, the substances present in body fluids that can serve as detecting diseases early, screening high-risk populations, monitoring drug therapy, and predicting recurrence.^{30,31} A greater number of articles have been published along with the knowledge on the clinical significance of serum proteins in the biological and medical applications. However, the analysis of serum proteins is extremely arduous and full of challenges, including the wide dynamic range of serum compounds, presence of high concentrations of salts, and interference of high-abundance proteins. More specifically, this annoying obstruction like albumin, which accounts for half of most proteins in serum,³² creates the masking effects to interrupt the detection of sparse biomarkers and reduces the specific sensitivity. In addition, high levels of salts probably affect the electrical characteristic of the sensor device as well as decrease the sensitivity of the nanowire sensor. For these reasons, we hereby developed a simple and convenient standard operating procedure for real-sample pretreatment. First of all, we used a microfilter (purchased from Sartorius Stedim Biotech) to remove the residual cells and purified the serum components. In the following, we chose the appropriate size of centrifugal filter (Sartorius Stedim Biotech, 3000 MWCO) for sample desalting, and then exchanged the buffer to control our experimental conditions. By means of these uncomplicated methods, analysis of low-abundance serum proteins becomes a more efficient and simpler way.

RESULTS AND DISCUSSION

Electrical Characteristics of Poly-Si NWFET Devices.

The typical electrical characteristics of a poly-Si NWFET device are shown in Figure 1b. The values of drain current can be controlled by the applied gate voltage. When the n-type FET is applied a gate voltage (V_{gs}) from negative bias to positive bias, the negative charges are induced in this channel. The p–n junction blocks the electrical current from drain to source, and there is an extremely low leakage current (I_{off}) in the level of picoamps by applying a smaller gate voltage. On the contrary, when the gate voltage is high enough to open a conductive channel between source and drain, the drain current increases sharply and the gate voltage is called threshold voltage. The n-type poly-Si NWFET has an excellent device performance, e.g., a high $I_{\text{on}}/I_{\text{off}}$ current ratio about 6 orders of magnitude. The drain current versus gate voltage output characteristics also depends on the controlled gate voltage, as shown in Figure 1c. It is found that the drain current exhibits pinch-off and current

saturation, indicating that the poly-Si NWFET follows standard FET characteristics. The $I_{ds}-V_{gs}$ and $I_{ds}-V_{ds}$ curves in aqueous solution shown in Figure 1, parts b and c, were similar to that obtained in air, respectively. Our results depict that the presence of the protection layers (100 nm wet oxide and 50 nm silicon nitride) can maintain a low gate leakage current, and this is especially important when a highly sensitive transducer is needed for the detection of analyte. Si substrate covered with the wet oxide and silicon nitride layers was employed to prevent the device from liquid invasion and keep its excellent electrical characteristics in aqueous solution.²⁷

Immobilization of IgG Fluorescence on Poly-Si Film Surface. In order to confirm the successful surface modification of a poly-Si NWFET device with APTES and glutaraldehyde, IgG labeled with a fluorescent dye was utilized. In the experiment, the fluorescent dye was applied with fluorescein isothiocyanate (FITC). We employed the fluorescence microscope (Olympus BX51) to observe the IgG immobilization of surface modification prepared under different conditions. The fluorescence images are shown in Figure 2.

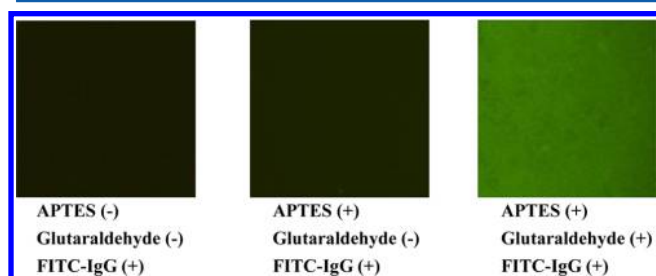


Figure 2. Fluorescent microscopic images of the poly-Si film surface following the hybridization with FITC-IgG. (a) Unmodified poly-Si film surface with FITC-IgG. (b) The surface of a poly-Si film modified with APTES. (c) The surface of a poly-Si film modified with APTES and glutaraldehyde.

These images are an extremely powerful evidence to illustrate the immobilization of the antibodies on the surface of a poly-Si film. The unmodified poly-Si film and the poly-Si film modified with APTES exhibited dark fluorescence as shown in Figure 2, parts a and b, respectively. Figure 2c depicts the expected fluorescent light for sample modified with APTES and glutaraldehyde due to the success of complete surface functionalization.

Electrical Responses of PSA with Various pH Buffers.

The device sensitivity and conductance changes depend on not only protein concentrations but also protein charges according to the aqueous solutions at various pH values. Protein such as PSA has a mildly acidic isoelectric point (pI) of ~ 6.9 , and hence the electrical response would probably reduce. For this reason, we employed the poly-Si devices to detect various PSA concentrations in different pH buffers and thus monitoring its electrical response. Initially, all samples were diluted in $0.01\times$ PBS buffer solutions,^{28,33} and then we chose the PBS buffer as a baseline to verify that there is no performance shift for subsequent measurements. Afterward, we switched the prepared samples to inject the sensing region and thus recorded these analytical data. The $I_{ds}-V_{gs}$ curves of a poly-Si NWFET biosensor for different PSA concentrations are shown in Figure 3a. Figure 3b depicts the relationship between the drain current and PSA concentration. For an n-type poly-Si NWFET biosensor, an increase of the drain current is attributed to the higher level of positive charges due to high PSA concentration with pH 6.2 less than 6.9. The plot of drain current versus logarithmic PSA concentrations exhibited a good linearity. On the contrary, the opposite results are shown in Figure 4, parts a and b. The augmented negative charges hindered the conducting channel of a poly-Si NWFET device and hence decreased the drain current when various PSA concentrations with pH 7.6 is higher than 6.9. According to the Langmuir isotherm model, the relation of association constant (K_A) is given by³⁴

$$\frac{\Delta I}{[C]} = K_A I_{\max} - K_A \Delta I \quad (1)$$

where $[C]$ is the analyte concentration in the PBS buffer, ΔI is the net change in the drain current at a given concentration $[C]$, and I_{\max} is the maximum net change in the drain current upon immunoreaction. The K_A values of 5.3×10^9 and $1.5 \times 10^{10} \text{ M}^{-1}$ were obtained for the pH 6.2 and the pH 7.6 analyte solutions, respectively, as shown in the inset of Figures 3b and 4b. These values are quite similar to the reported values measured for immunoreactions between PSA and anti-PSA.³⁴ As mentioned above, the poly-Si NW devices were functionalized APTES, glutaraldehyde, and anti-PSA before utilization for biosensing application. All data were measured three times to confirm the complete reactions and avoid the errors. These

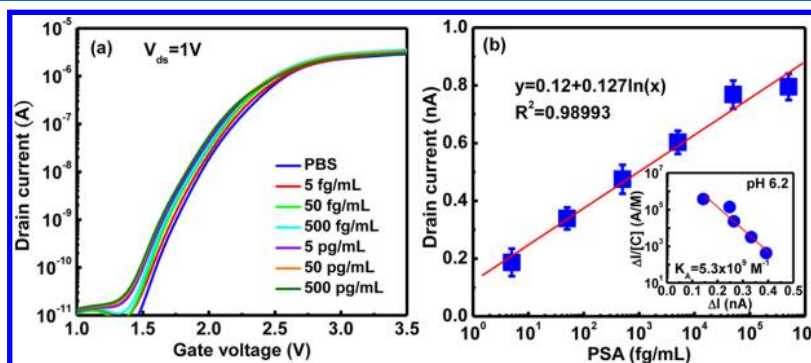


Figure 3. Electrical responses of the poly-Si NWFET device for various PSA aqueous solutions (pH < pI). (a) The $I_{ds}-V_{gs}$ curve of the baseline (blue line) was obtained in PBS buffer; these electrical responses of a biosensor device showed the expected shift for PSA concentration from 5 fg/mL to 500 pg/mL. (b) Drain current ($V_{gs} = 1.6 \text{ V}$) as a function of PSA concentration. The inset to panel b depicts the plot of $\Delta I/[C]$ against ΔI at different PSA concentrations according to the Langmuir isotherm model, thus gives a straight line from which K_A can be calculated.

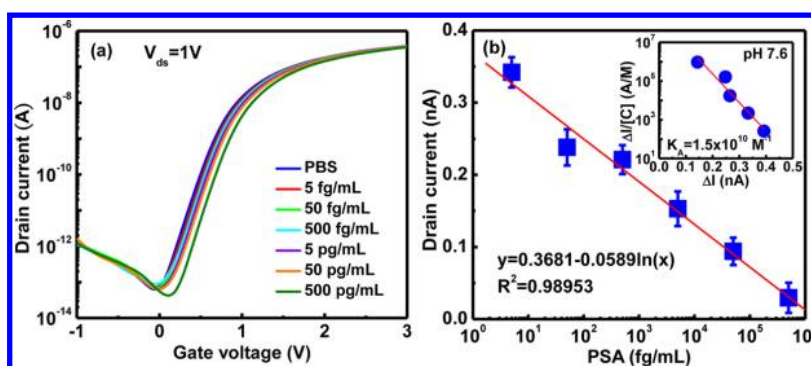


Figure 4. Electrical responses of the poly-Si NWFET device for different PSA aqueous solutions ($\text{pH} > \text{pI}$). (a) This $I_{\text{ds}}-V_{\text{gs}}$ curve of the baseline (blue line) was recorded in PBS buffer; buffer solutions with various PSA concentrations were injected to the sensor area. (b) Drain current ($V_{\text{gs}} = 0.6 \text{ V}$) of the poly-Si NWFET sensor plotted with respect to the PSA concentration. The inset to panel b shows the $\Delta I/[C]$ as a function of ΔI . The straight line illustrates the fitting result from eq 1 with the association constant $K_{\text{A}} = 1.5 \times 10^{10} \text{ M}^{-1}$ at $\text{pH} 7.6$.

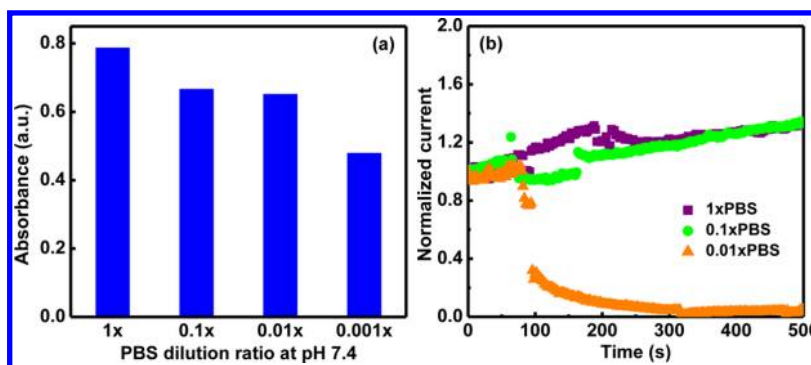


Figure 5. (a) ELISA absorbance value plotted vs the PSA concentration with different diluted PBS buffer solutions. (b) Electrical responses of a poly-Si NWFET sensor for various diluted PBS buffer solutions. The sample with 0.01 \times PBS solution showed electrical response (orange line). In contrast, the PSA with 1 \times and 0.1 \times PBS solutions had no electrical response because of the insufficient Debye length.

results indicated that this poly-Si NW sensor device has the potential to screen men for prostate cancer.

Detection of PSA with Various Diluted PBS Solutions.

The binding of charged molecules on a sensor surface alters the carrier density in it through electrostatic gating and/or charge transfer, causing the changes in the direct current conductance of the FET device. However, the detecting charges in high ionic strength solutions are fundamentally hindered by ionic screening.^{28,33} The parameter of Debye length plays an important role in electrolytes to affect the FET device performance. The Debye length with 1 \times , 0.1 \times , 0.01 \times , and 0.001 \times PBS buffer solutions was evaluated to be ~ 0.7 , ~ 2.4 , ~ 7.5 , and $\sim 23.9 \text{ nm}$, respectively, using the formula²⁸ $\lambda_{\text{D}} = 0.32(I)^{-0.5}$, where I is the ionic strength of the buffer solution. The Debye length is the distance over which significant charge separation can occur; that is, a longer Debye length is expected to be long enough to guarantee less charges screened by using a dilute buffer solution with low electrolyte concentrations. In order to utilize a sufficient and reasonable Debye length, the biological FET sensor system should be conducted in buffer solutions with low salt concentrations. However, the interaction between the antigen and antibody is a bimolecular association and requires salts to maintain this bond stability. To verify the capability of protein–protein binding under low-salt conditions, we employed the ELISA kit to demonstrate the results (Figure 5a). The data indicated that the association between antigen and antibody was still good in spite of the dilution PBS solution (up to 0.01 \times dilution ratio). In comparison with a lower dilution ratio, the ELISA absorbance value of protein complex

with 0.001 \times PBS solution depressed obviously due to the scarce salt.

To evaluate the impact of Debye length screening on PSA sensing, we also measured the $I_{\text{ds}}-V_{\text{gs}}$ curves (Figure 5b). For the influence of varying ionic concentrations on biological measurement sensitivity, 50 pg/mL PSA in 1 \times , 0.1 \times , and 0.01 \times PBS solutions was prepared. An obviously normalized current alteration in electrical detection was found in the 0.01 \times PBS solution. This is because Debye length ($\sim 7.5 \text{ nm}$) of this 0.01 \times PBS solution is larger compared to the length of $\sim 4.2 \text{ nm}$ for the PSA antibody.³⁵ In other words, the Debye length is sufficiently long to achieve accurate screening and effective detection. However, the biological analytes in 1 \times and 0.1 \times PBS solutions could not see the detectable signals because of their shorter Debye length. The poly-Si NWFET sensors were modified with APTES and glutaraldehyde as a linker to connect to the anti-PSA for specificity before electrical measurements.

Detection of Various PSA Concentrations. Tumor markers are substances that can be found in the blood, urine, stool, other bodily fluids, or tissues of some patients with cancer. Most tumor markers are proteins and are made by normal cells as well as by cancer cells; however, they are produced at much higher levels in cancerous conditions. Early detection is finding cancer at an early stage, when it is less likely to have spread and is easier to treat. The PSA test is used to screen men for prostate cancer. Men with prostate cancer usually have high PSA levels. It is undoubtedly true that rapid screening and real-time detection of trace biomarkers in human serum are especially important in medical applications. As a

consequence, we employed the poly-Si NWFET device with excellent electrical performance to perform the measurement of PSA in desalted human serum. The samples of raw human serum were collected from healthy individuals and then pretreated by filtration, desalting, and buffer exchange. Different quantities of PSA were added into the desalted serum to obtain the required concentration of sample solutions.

In order to reduce the nonspecific binding of nontarget proteins, we utilized Tween 20³⁶ and an amphipathic polymer to serve as the passivation agent by immobilization on the poly-Si NWFET. Tween 20 is a detergent and usually plays a role as blocking agent in bioanalytical assays such as Western blot for reduction of nonspecific binding to decrease the background signal. The normalized current versus time for the poly-Si NWFET device passivated with Tween 20 after the anti-PSA functionalization step is revealed in Figure 6. The desalted

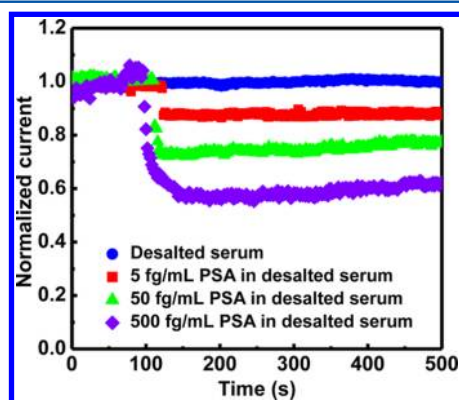


Figure 6. Normalized current of poly-Si NWFET devices immobilized with PSA antibodies to screen various PSA concentrations in desalted human serum. Desalted serum without PSA exhibited no electrical response.

serum solution without PSA was injected into the sensor region to establish an initial baseline, and the drain current of the device immediately dropped down subsequent to the addition of PSA in the serum solution. The serum solution with 500 fg/mL PSA concentration is more obvious electrical response compared to 5 fg/mL PSA concentrations, as shown in Figure 6. The detection results demonstrated the success in real-sample application by employing the novel poly-Si NWFET. Consequently, this nanosensor has great potential to be developed as a diagnostic platform for monitoring prostate cancer and predicting the risk of early relapse after radical prostatectomy.

CONCLUSIONS

We have demonstrated a simple and low-cost method for poly-Si NWFET fabrication having excellent electrical characteristics, ultrahigh sensitivity, and specificity. The manufacturing process of our device was advantageous to mass production because of its replacement for expensive materials and processes. The electrical performance of the poly-Si NWFET device exhibited 6 orders of magnitude on I_{on}/I_{off} current ratio. We have successfully screened an ultratrace PSA tumor marker at femtogram level in not only $0.01\times$ PBS buffer solution but also desalted human serum by employing this functionalized nanosensor. In this study, we developed a convenient and uncomplicated standard operating procedure to achieve the pretreatment of human serum by utilizing Tween 20,

suppressing the influence in signal detection of target analytes. Our approach provides a real-time and label-free diagnostic platform for multiple chemical and biological species. Therefore, this biosensor appears to be a very promising candidate for screening diseases in the earliest stages, assessing and monitoring medication therapy, as well as predicting the recurrence rate after treatment in the foreseeable future.

AUTHOR INFORMATION

Corresponding Author

*Phone: 886-3-211-8800, ext 3349 (T.-M.P.); +886 35712121, ext 55803 (F.-H.K.). Fax: 886-3-211-8507 (T.-M.P.); +886 3 5729912 (F.-H.K.). E-mail: tmpan@mail.cgu.edu.tw (T.-M.P.); fhko@mail.nctu.edu.tw (F.-H.K.).

Notes

The authors declare no competing financial interest.

ACKNOWLEDGMENTS

The authors thank the Chang Gung Memorial Hospital and the National Science Council of the Republic of China, Taiwan, for financially supporting this research under contracts CMRPD290031, 290032, and 290033, and NSC 101-2113-M-009-007-MY3, respectively.

REFERENCES

- (1) Siegel, R.; Naishadham, D.; Jemal, A. *CA—Cancer J. Clin.* **2012**, *62*, 10–29.
- (2) Garnick, M. B. *Ann. Intern. Med.* **1993**, *118*, 804–818.
- (3) Stone, J. G.; Rolston, R. K.; Ueda, M.; Lee, H. G.; Richardson, S. L.; Castellani, R. J.; Perry, G.; Smith, M. A. *Int. J. Clin. Exp. Pathol.* **2009**, *2*, 267–274.
- (4) Webber, M. M.; Waghray, A.; Bello, D. *Clin. Cancer Res.* **1995**, *1*, 1089–1094.
- (5) Catalona, W. J.; Smith, D. S.; Ratliff, T. L. *N. Engl. J. Med.* **1991**, *324*, 1156–1161.
- (6) Oesterling, J. E. *J. Urol.* **1991**, *145*, 907–923.
- (7) Benson, M. C.; Whang, I. S.; Olsson, C. A. *J. Urol.* **1992**, *147*, 817–821.
- (8) Nagel, B.; Dellweg, H.; Gierasch, L. M. *Pure Appl. Chem.* **1992**, *64*, 143–168.
- (9) Ivnitski, D.; Abdel-Hamid, I. *Biosens. Bioelectron.* **1999**, *14*, 599–624.
- (10) Cecilia, J. J.; Jahir, O.; Antoni, B. *Sensors* **2010**, *10*, 61–83.
- (11) Patolsky, F.; Zheng, G.; Liber, C. M. *Nat. Protoc.* **2006**, *1*, 1711–1724.
- (12) Ray, S.; Mehta, G.; Srivastava, S. *Proteomics* **2010**, *10*, 731–748.
- (13) Brennan, D. J.; Fagan, A. *Expert Opin. Biol. Ther.* **2005**, *5*, 1069–1083.
- (14) Liu-Stratton, Y.; Roy, S.; Sen, C. K. *Toxicol. Lett.* **2004**, *150*, 29–42.
- (15) Ward, A. M.; Catto, J. W. F.; Hamdy, F. C. *Ann. Clin. Biochem.* **2001**, *38*, 633–651.
- (16) Rich, R.; Myszk, D. G. *Curr. Opin. Biotechnol.* **2000**, *11*, 54–61.
- (17) Kim, N.; Kim, D. K.; Cho, Y. J. *Sens. Actuators, B* **2009**, *143*, 444–448.
- (18) Backmann, N. *Proc. Natl. Acad. Sci. U.S.A.* **2005**, *102*, 14587–14952.
- (19) Waggoner, P. S.; Varshney, M.; Craighead, H. *Lab Chip* **2009**, *9*, 3095–3099.
- (20) Zheng, G.; Gao, X. P. A.; Liber, C. M. *Nano Lett.* **2010**, *10*, 547–552.
- (21) Chen, K. I.; Li, B. R.; Chen, Y. T. *Nano Today* **2011**, *6*, 131–154.
- (22) Lin, H. C.; Lee, M. H.; Su, C. J. *IEEE Electron Device Lett.* **2005**, *26*, 643–645.

- (23) Su, C. J.; Lin, H. C.; Huang, T. Y. *IEEE Electron Device Lett.* **2006**, *27*, 582–584.
- (24) Su, C. J.; Lin, H. C.; Tsai, H. H.; Wang, T. M.; Huang, T. Y.; Ni, W. X. *Nanotechnology* **2007**, *18*, 215205.
- (25) Lin, C. H.; Hsiao, C. Y.; Hung, C. H. *Chem. Commun.* **2008**, *44*, 5749–5751.
- (26) Hsiao, C. Y.; Lin, C. H.; Hung, C. H. *Biosens. Bioelectron.* **2009**, *24*, 1223–1229.
- (27) Lin, C. H.; Hung, C. H.; Hsiao, C. Y.; Lin, H. C.; Ko, F. H.; Yang, Y. S. *Biosens. Bioelectron.* **2009**, *24*, 3019–3024.
- (28) Chua, J. H.; Chee, R. E.; Agarwal, A. *Anal. Chem.* **2009**, *81*, 6266–6271.
- (29) Pound, C. R.; Partin, A. W.; Eisenberger, M. A. *JAMA, J. Am. Med. Assoc.* **1999**, *281*, 1591–1597.
- (30) Ebert, M. P.; Korc, M.; Malfertheiner, P. *J. Proteome Res.* **2006**, *5*, 19–25.
- (31) Ray, S.; Reddy, P. J.; Jain, R. *Proteomics* **2011**, *11*, 2139–2161.
- (32) Anderson, N. L.; Anderson, N. G. *Mol. Cell. Proteomics* **2002**, *1*, 845–867.
- (33) Stern, E.; Wagner, R.; Sigworth, F. J. *Nano Lett.* **2007**, *7*, 3405–3409.
- (34) Lin, S.; Lee, A. S. Y.; Lin, C. C.; Lee, C. K. *Curr. Proteomics* **2006**, *3*, 271–282.
- (35) Erickson, H. P. *Biol. Proced. Online* **2009**, *11*, 32–51.
- (36) Chang, H. K.; Ishikawa, F. N.; Zhang, R. *ACS Nano* **2011**, *5*, 9883–9891.